Glass Technol.: Eur. J. Glass Sci. Technol. A, December 2013, **54** (6), 211–217

Comparison of the mechanical and tribological properties of a sintered low expansion Li_2O–Al_2O_3–SiO_2 glass-ceramic and a commercial cooktop plate

Silvio Buchner,[a,*] *Viviane Oliveira Soares,*[b] *Paulo Soares,*[c] *Carlos M. Lepienski*[d] *& Edgar D. Zanotto*[e]

[a] *High Pressure and Advaced Materials (LAPMA), Physics Institute, Universidade Federal do Rio Grande do Sul, CP 15051, 91501-970 Porto Alegre – RS, Brazil, silviobuchner@gmail.com; silvio.buchner@ufrgs.br*
[b] *Departament of Science, Universidade Estadual de Maringá, 87360-000 Goioerê – PR, Brazil*
[c] *Department of Mechanical Engineering, Polythecnic School, Pontifícia Universidade Católica do Paraná, 80215-901 Curitiba – PR, Brazil*
[d] *Physics Department, Universidade Federal do Paraná, 81531-990 Curitiba – PR, Brazil*
[e] *Vitreous Materials Laboratory (LaMaV), Department of Materials Engineering, Universidade Federal de São Carlos, 13565-905 São Carlos – SP, Brazil (lamav.weebly.com)*

Manuscript received 6 March 2013
Revision received 12 June 2013
Manuscript accepted 13 June 2013

The mechanical and tribological properties of a new sintered lithium aluminium silicate (LAS) glass-ceramic were compared to those of a commercially Ceran® used in cooktops. The sintered material has no nucleating agents and was obtained by viscous sintering with concurrent surface crystallisation of a glass powder compact whereas the Ceran sample was cut from a plate produced by Schott in the traditional way. Tribological experiments were carried out using a tribometer with reciprocating sliding ball-on-flat method in two controlled conditions: namely 52% relative humidity at 23°C and with running water at 23°C. The sintered glass-ceramic has a hardness of H_{IT}*=8·3±0·4 GPa and elastic modulus of* E_{IT}*=79±2 GPa, whereas the commercial Ceran has a hardness of* H_{IT}*=9·1±0·2 GPa and an elastic modulus of* E_{IT}*=85±1 GPa. The tribological tests in dry conditions revealed that the sintered glass-ceramic has slightly lower wear rates than Ceran. Under wet conditions both materials had lower friction coefficients than in dry conditions, but their wear rates were higher. Based on the results plus an additional thermomechanical evaluation (reported in another article), we suggest that this new sintered GC could be an alternative, suitable material for cooktops.*

1. Introduction

Glass-ceramics (GC) are polycrystalline materials obtained by the controlled crystallisation of suitable glasses during heat treatment processes.[1] They usually contain one or more crystalline phases and a residual glass phase. The types of crystal phases, crystallised fraction, crystal size distributions and crystal morphologies control most of the properties including wear resistance, hardness, refractoriness, chemical resistance, dimensional stability, optical and electrical properties.[2]

Li_2O–Al_2O_3–SiO_2 (LAS) glass-ceramics were among the first to be developed, but they still have high commercial value due to their excellent chemical durability, and refractoriness up to 700°C combined with ultra-low thermal expansion, which leads to great thermal shock resistance.[3] They are commonly used as cooktop plates, telescope mirrors and high temperature windows.[4–6] The low thermal expansion coefficient of these materials is due to the presence of some crystalline phases that exhibit highly anisotropic thermal expansion coefficients (TEC), such as β-quartz solid solutions.[7] The slightly positive TEC of the residual glassy phase combined with the (overall) negative TEC of the crystalline phase results in ultra-low thermal expansion glass-ceramics.

Commercial LAS glass-ceramics are produced by regular glass melting-forming techniques using compositions that contain one or more nucleating agents, such as TiO_2 and ZrO_2, followed by (internal) nucleation and crystallisation heat treatments.[8] An alternative route to produce glass-ceramics is to use glass powder compacts of nucleant free compositions, followed by appropriate thermal treatments to induce simultaneous viscous flow sintering and surface crystallisation of the glass particles.[9] The interplay between the densification and surface crystallisation kinetics may result in a variety of microstructures with different porosities and crystalline fractions.[10] For instance, if surface crystallisation takes place in

[1] Corresponding author. Email silviobuchner@gmail.com; silvio.buchner@ufrgs.br

the early stages of sintering, viscous flow is hindered and a highly porous body is obtained.[11,12] Therefore, glasses that easily crystallise are not suitable to achieve high densification (low porosity) by this method.[13] In a previous paper, the best sintering conditions for the same GC analysed in this paper were determined, resulting in a sintered glass-ceramic with less than 5% residual porosity and a ultra low thermal expansion coefficient of 2×10^{-8} °C^{-1}.[14,15]

From the engineering applications standpoint, extensive emphasis has been given to the mechanical properties of glass-ceramics. Their flaw propagation resistance is one of the most important,[1] whereas the other relevant point is wear resistance.

The indentation technique has been used for the determination of the hardness (H) and elastic modulus (E) of glasses and glass-ceramics.[16–20] The interest in this technique has grown in the last years due to the development of instrumented indenters at nanoscale, also known as nanoindenters[21] and the improvement of the procedures for measuring these properties, with the possibility of mapping the surface properties with micrometer resolution.[22] Nanoindenters continuously measure the force and displacement during penetration allowing for the simultaneous determination of the elastic modulus, fracture toughness and hardness.[23]

Besides these properties, the wear resistance is also of great interest for some applications. For instance, Gant & Gee[24] studied the effect of tribo-chemical reaction on the sliding wear of ceramics. According to these authors the wear of a ceramic material is affected by a synergy of sliding wear and corrosion by the fluid. When tribological tests are performed under running water, a continuous dissolution of the surface occurs by a tribochemical reaction between the glass and crystal phases and water.[25,26] The interaction between SiO_2 and water produces structural and chemical changes that alter the chemical composition and pH on the material's surface. According to several authors,[e.g. 27] the reaction between a soda–lime–silica glass and water happens in two stages. In the primary stage there is a substitution of the sodium ions by hydrogen ions from the water; in this stage there is no interaction between Si–O–Si bonds and hydrogen. In the second stage there is a breakdown of the Si–O–Si bonds and partial or total glass dissolution in the aqueous solution.

The Archard coefficient (K) is used to describe sliding wear and is based on the theory of asperity contact (please consult Stachowiak *et al*[28] for details). The Archard coefficient can also be seen as the amount of asperity contacts resulting in wear. The value of K is never supposed to exceed unity and it has a value of 10^{-3} or less for the most severe forms of wear. A low value of K indicates that wear is caused by a small amount of asperity contacts.[28]

The specific wear rate (W) is defined by[29,30]

$$W = \frac{V}{PL} \tag{1}$$

where W has units of volume loss per unit of force per unit of distance (mm^3/Nm), P is the normal load, L the sliding distance and V is the calculated volume assuming an elliptical wear profile, which is determined by the expression

$$W = \frac{\pi whl}{2} \tag{2}$$

where w is the wear groove width (semi-minor axis), h is the wear groove depth (semi-major axis) and l is the wear track length.

The Archard coefficient (K) is the proportionality constant between the real contact area, sliding distance and the wear volume[19,28,31,32]

$$V = KA_rL = \frac{KLP}{H} \tag{3}$$

where V is the volume loss, A_r is the real contact area, L is the sliding distance, P is the applied load and H is the hardness of the softer surface.

Buchner *et al*[19] investigated the friction coefficients, wear rate and Archard coefficient of a sintered glass-ceramic (cristobalite (SiO_2) and devitrite $Na_2O.3CaO.6SiO_2$), compared to granite and porcelainised stoneware in wet and dry conditions. It was shown that the tribological behaviours of these materials change with the test condition. The wear rate and the Archard coefficient were higher in the wet-conditions than in the dry conditions for the three tested materials. The wear rates (in mm^3/Nm) for the dry condition were 0·2 for the glass-ceramic, 0·9 for the porcelainised stoneware, and 407 and 0·7 for the granite [region 1 (mica) and region 2 (quartz+feldspar)], respectively. For wet-conditions, the values were 9 for the glass-ceramic, 5 for the porcelainised stoneware, 632 and 8 for the mica and quartz+feldspar granite regions, respectively.[19] The Archard coefficients (in multiples of 10^{-3}) for dry and wet conditions were: 0·0013 and 0·0565 for the glass-ceramic, 0·0056 and 0·0327 for the porcelainised stoneware, 0·6513 and 1·0118 for the mica region of the granite, 0·0065 and 0·0713 for the feldspar+quartz region of the granite,[19] respectively.

The aim of this work was to evaluate and compare the hardness, elastic modulus and tribological behaviour of a new lithium aluminium silicate (LAS) glass-ceramic produced by viscous sintering with concurrent crystallisation of glass powder compacts, with those of the commercial Ceran used in cooktops.

2. Experimental procedure

2.1. Sintered glass-ceramic preparation

A specially designed lithium aluminium silicate glass was obtained from analytical grade Li_2CO_3, Al_2O_3, SiO_2 and other minor components: K_2CO_3, MgO, ZnO,

$BaCO_3$, P_2O_5, H_3BO_3, SnO_2 and As_2O_3. The chemical composition of the commercial GC Ceran is presented in Guedes *et al.*[33] The chemical composition of the sintered LAS GC was (mol%): 67·3SiO_2, 15·6Al_2O_3, 8·4 Li_2O, 1·6MgO, 0·8ZnO, 2·0P_2O_5, 1·4B_2O_3, 0·9K_2O, 0·6SnO_2, 1·1BaO, 0·3As_2O_3. The mixture of precursor powders was homogenised and melted in a platinum crucible at 1600°C for 3 h in an electric furnace in air. The melt was quenched into water and the 'frits' were crushed in a Fritsch Pulverisette high impact ball mill. After adequate sieving, the particle sizes ranged from 0·2–60 μm.

Cylinders (diameter 20 mm, height 4 mm) were formed by uniaxially pressing the glass powder at 60 MPa with 2 wt% oleic acid. Sintered LAS glass-ceramics were submitted to an initial heat treatment at 500°C for 120 min in an electric furnace to remove the binder. They were then heated at 30°C/min up to 1000°C without any holding time. Finally, they were cooled inside the furnace with an average cooling rate of 15°C/min. The samples were ground on SiC paper and subsequently polished in a suspension of CeO_2. The porosity was determined by optical microscopy (Leica DM-RX with a CCD camera DFC 490) using the image analysis software Image-J. As received commercial Ceran® samples were analysed in the same way.

2.2. Hardness and elastic modulus

The hardness and elastic modulus were obtained by instrumented indentation, where an indenter of known geometry is pressed into the material and the penetration depth (h) is continuously recorded as a function of the applied load (P) for both the loading and unloading cycles.[34–36] We used a XP Nanoindenter (MTS) with a Berkovich indenter tip (three sided diamond pyramid) with the area function calibrated using fused silica, applied loads from 3 to 400 mN, corresponding to eight complete loading-unloading cycles. Thirty-six indentations (6×6) separated by a distance of 150 μm were made, and the results are the average of these indentations. The hardness (H_{IT}) and elastic modulus (E_{IT}) from the P–h curves were determined by the Oliver and Pharr method.[34]

2.3. Tribological properties

The tribological properties were obtained using the ball-on-flat reciprocating sliding method[31] in a tribometer (CSM), using a tungsten carbide (WC) ball 6·3 mm in diameter. A WC ball was chosen as the counterface because it provided a necessary wear severity that would facilitate comparison of the materials wear resistance. We used the following conditions: applied load of 5 N, track length of 2 mm, with a sliding speed of 2 cm/s and total sliding distance of 20 m. The reciprocating sliding tests were conducted under two different controlled environmental conditions: 53 % relative humidity at 23°C and under running distilled water at 23°C. These two conditions are named dry and wet conditions, respectively, and three experiments were realised for each condition. The friction coefficient (μ) was continuously monitored during the experiments. The cross sectional profiles of the wear tracks were determined by the nanoindenter in the profilometry mode with a Berkovich tip and are the average of three measurements made at the centre of each track.

3. Results and discussion

The hardness and elastic modulus as a function of tip penetration depth for each material are shown in Figures 1 and 2, respectively.

The average values of hardness (H_{IT}) are 8·3±0·4 GPa for the sintered GC and 9·1±0·2 GPa for Ceran. The elastic modulus (E_{IT}) are 79±2 GPa for the sintered GC and 85±1 GPa for Ceran. Therefore the average values of H_{IT} and E_{IT} for the sintered GC are somewhat lower, but almost equivalent to those of Ceran.

It is well known that hardness, measured by a pointed indenter at small depths of penetration, often increases with decreasing depth of penetration. This effect is termed as the indentation size effect (ISE).[37] In brittle materials, the measurement of hardness is influenced by the presence of defects in the contact region. These defects can be present from manufacture or formed during indentation. For smaller applied loads, i.e. small tip contact area, less defects are present (or even none), and a higher contact pressure is necessary, resulting in higher hardness values.

According to Chakraborty *et al*,[38] depending on the presence or absence of microstructural defects, the specimens may exhibit both mild and strong ISE based on the premise that the deformation process

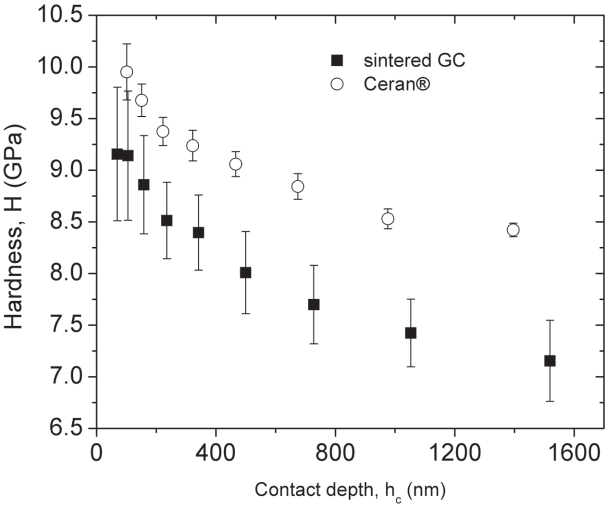

Figure 1. Hardness as a function of contact depth of the (■) sintered glass-ceramic and the (○) commercial glass-ceramic (Ceran)

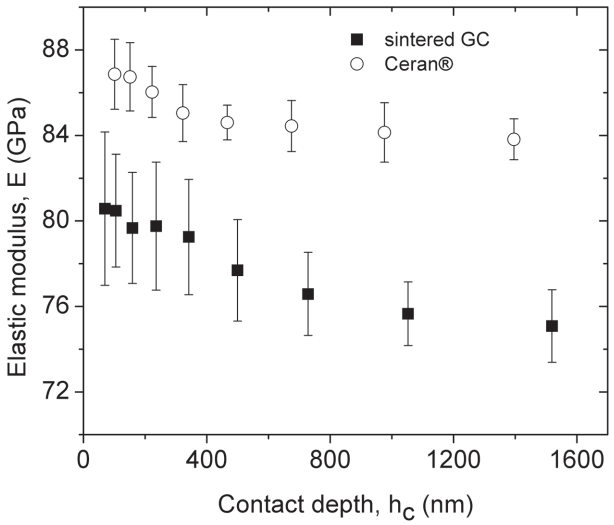

Figure 2. Elastic modulus as a function of contact depth of the (■) sintered glass-ceramic and the (o) commercial glass-ceramic (Ceran)

is controlled by formation, storage, and movement of dislocations.

Sample surfaces can also become harder due to residual stresses caused by crystallisation. Serbena *et al*[15] investigated the internal residual stresses in Ceran and in the same sintered GC studied in this work. Those authors reported that the same crystalline phase is formed in both glass-ceramics, but the composition and volume percentage of the residual glassy phases are distinct. Whereas in Ceran about 30 vol% residual glassy phase is present, in our sintered GC only 5–10 vol% residual glass reaches is present. The large amount of residual glass in Ceran may be responsible for its (slightly) smaller friction coefficient in the dry conditions. In the sintered GC the residual glass is not homogeneously distributed around the crystals. The original glass particles show a large size distribution ranging from a few nanometres up to 60 μm. After the sinter-crystallisation process, the interiors of the largest glass particles remain vitreous resulting in isolated portions of the glass phase, with an average size of about 11 μm. These glass phase regions and porosity contribute to decreasing the average values of hardness and elastic modulus for the sintered GC, since the measurements were taken in random regions of the sample. Further information about processing and microstructural characterisation of this sintered GC can be found in Soares *et al*.[39]

Another reason for the increase of hardness and elastic modulus with decreasing depth of penetration is the bluntness of the tip of the indenter. As a consequence, the actual contact area for very small distances from the tip is much larger than at the same distance for an ideal indenter. For a given load, the penetration of a real indenter is therefore smaller, and the hardness and modulus appears to be higher. With increasing depth, the influence of the tip bluntness becomes smaller and the measured hardness values gradually approach those for the ideal shape. It could be assumed that this is the case, where the tip area was calibrated to the average H_{IT} and E_{IT} of fused silica. Therefore, there is a combination of factors affecting the hardness and elastic modulus curves namely the contribution of residual stresses and calibration error.; the ISE affects only the hardness values.

The friction coefficient as a function of sliding distance is shown in Figure 3 (dry conditions) and Figure 4 (wet conditions). Three different regimes are identified for all friction coefficient profiles: (a) the running-in regime (accommodation between surface and ball); (b) the transition regime (complex mechanisms of fracture and deformation); and (c) the stationary regime (material removal at a constant rate).[31,40] In the running-in regime, the WC ball has low interaction with the sample; then there is only a first contact with the GC surface on the asperities and these asperities do not plastically deform. The stationary regime is characterised by a three body complex interaction involving the sample, the WC ball and the debris formed by particle fracture and delamination.

The average friction coefficient (μ) was determined in the stationary regime (sliding distance > 3 m) in dry conditions (Figure 3) for both samples. The stationary regime was reached in a continuous way for the new GC, while the commercial sample presented an abrupt increase of the friction coefficient between 0·15 and 0·40 m, however, it only reached the stationary regime after around 3 m.

A completely different behaviour was observed when the tribological tests were performed under running water (Figure 4). No stationary regime was reached for Ceran, which means that there is a similar dissolution of the surface in the aqueous solution (0<sliding distance<15 m), due to tribochemical reactions of the glassy phase with water.[25,26] Around 15–15·8 m there was a decrease of the friction coef-

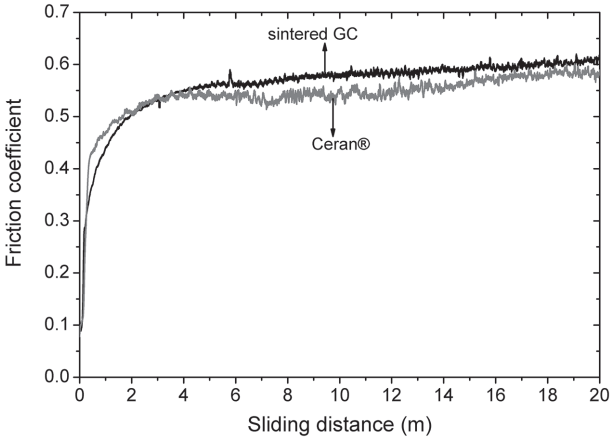

Figure 3. Friction coefficient profiles of samples tested at 53% relative humidity (dry) at 23°C with an applied load of 5 N. The total scratch length was 20 m

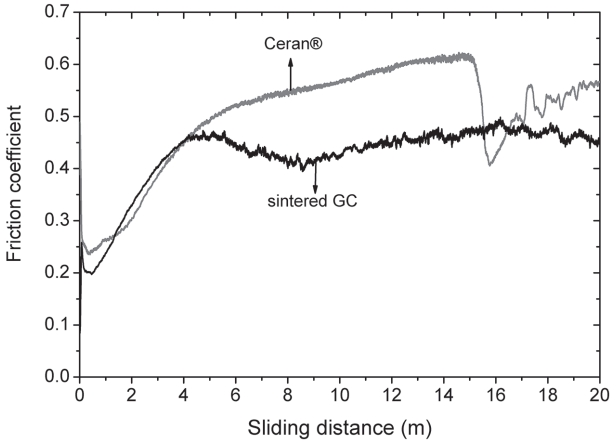

Figure 4. Friction coefficient profiles of samples tested with running distilled water (wet) at 23 °C with an applied load of 5 N. The total scratch length was 20 m

ficient of Ceran. Soon after this event the friction coefficient started to increase, but did not reach the stationary regime up to 20 m. It is known that the interaction between SiO_2 in the material and water produces structural and chemical changes that alter the chemical composition and pH on the surface.[27]

For the experiment in wet conditions, the sintered GC reached the stationary regime in a monotonic way (Figure 4). In this case the stationary regime was reached after about 4·2 m. The decrease in the friction coefficient around 5–10 m is due to the lubricating effect of the material extracted in the initial stage. During the initial stage (accommodation between surface and ball[31,40]) and the transition regime (complex mechanisms of fracture and deformation[31,40]) significant interaction between the WC ball and the surface of the samples occurs. Fracture and deformation of the surface take place in these stages and a portion of material is removed at a non-constant rate. Part of the material removed along with water, probably acts as a lubricant in the following stages contribuing to the approach to the stationary regime. Figures 5(a) and (b) show the groove profiles obtained in the centre of the wear tracks for both test conditions, dry (53% relative humidity) and wet (running water) at 23°C, respectively.

The grooves of both materials are similar, as shown in Figure 5(a). When these materials were submitted to the same test in running water (see Figure 5(b)) the groove sizes increased for both. The specific values of wear rate in the dry condition were $10{\cdot}5\times10^{-6}$ $mm^3/(Nm)$ for Ceran and $8{\cdot}4\times10^{-6}$ $mm^3/(Nm)$ for the sintered GC. Hence, in this condition, the wear rate of the sintered GC was about 20% smaller than that of Ceran. The specific values of wear rate in the wet condition were about 60×10^{-6} $mm^3/(N.m)$ for both glass-ceramics.

The Archard coefficient is typically reported in multiples of 10^{-3}.[17,29,35] In the dry conditions, the Archard coefficients were $0{\cdot}0895\times10^{-3}$ and $0{\cdot}0608\times10^{-3}$

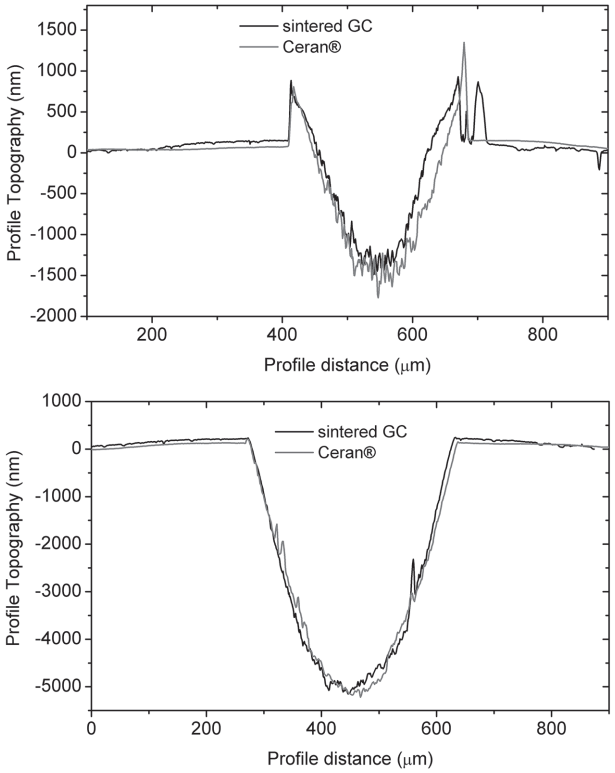

Figure 5. Groove profiles obtained in the centre of the wear track for test conditions, a) dry (53% relative humidity at 23 °C). b) Groove profiles obtained in the centre of wear track for wet test conditions (running distilled water at 23 °C)

for Ceran and the sintered GC, respectively. In the wet conditions, the Archard coefficients were $0{\cdot}5057\times10^{-3}$ for Ceran and $0{\cdot}4338\times10^{-3}$ for the sintered GC. Therefore, the sintered GC has a slightly smaller Archard coefficient than that of Ceran. The lower value of the Archard coefficient (K) indicates that wear is caused by a quite small number of asperity contacts.[28]

The porosity (determined by optical microscopy) of the sintered GC is 5±1%, whereas the commercial GC Ceran has a pore-free surface. Hence the variations observed in mechanical properties can be associated with the different surface qualities of the two glass-ceramics. The sintered GC has a lower elastic modulus probably due to its porosity.

The present results show that the sintered GC and Ceran have similar friction coefficients in dry conditions, and that the wear rate is somewhat smaller for the sintered GC. The sintered GC presents lower coefficients of friction when immersed into water. The commercial GC plate shows a sharp decrease in the friction coefficient after about 15 m in wet conditions. The results of profile topography indicate a greater wear for both samples when immersed in water when compared to dry conditions. Considering the wet conditions, the sintered GC presents a lower coefficient of friction than Ceran. However, Ceran shows a sharp decrease in the coefficient of friction after about 15 m.

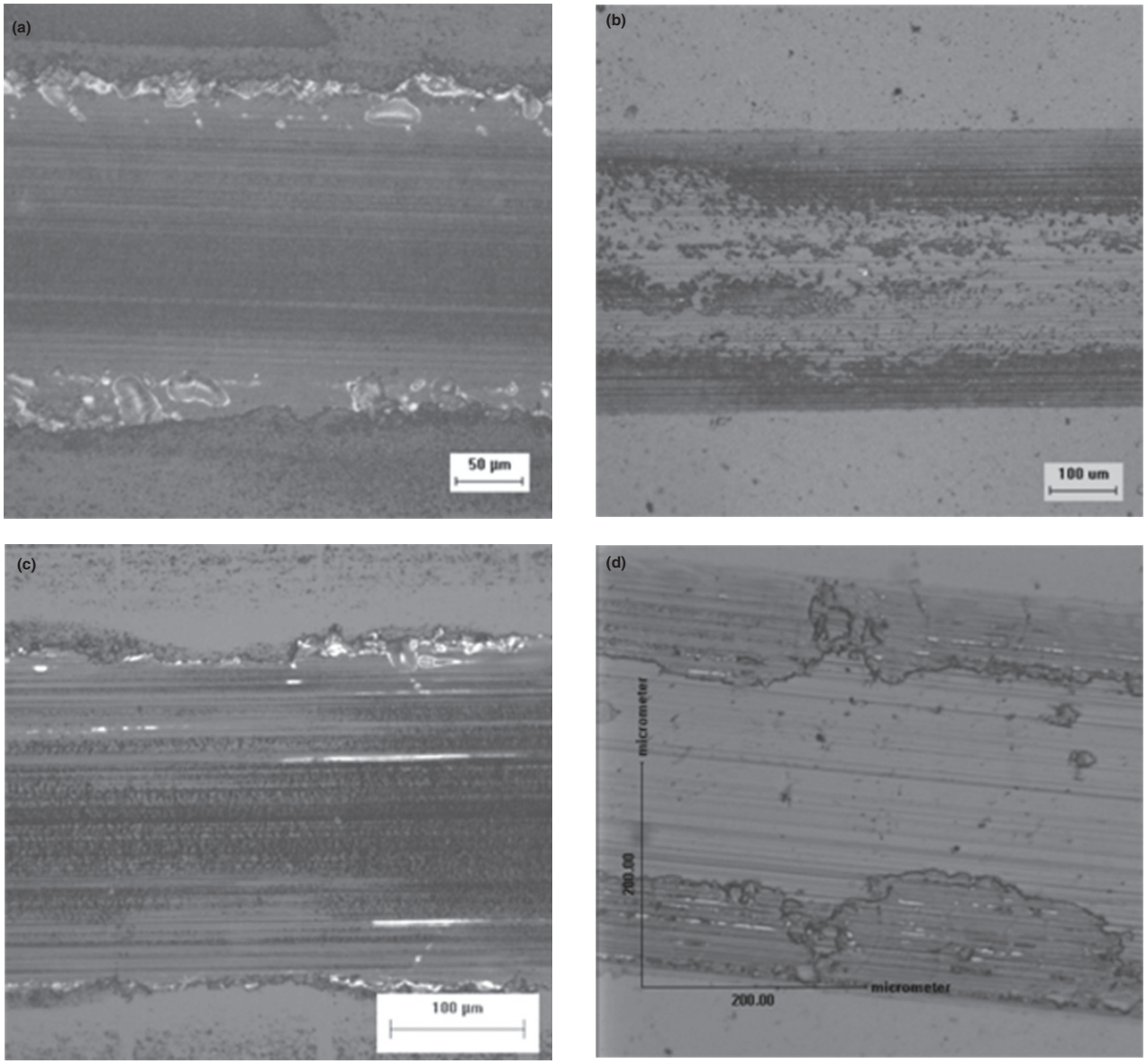

Figure 6. Optical micrographs of the wear track for both test conditions, dry and wet. (a) Sintered GC – Dry; (b) Sintered GC – Wet; (c) Ceran – Dry; (d) Ceran – Wet

Figure 6 shows that the surfaces after tribological testing, for different experimental conditions.

As can be seen in Figure 6, samples tested under dry conditions have a relatively smoother surface. In the wet conditions wear was more severe resulting in a deeper wear grooves as observed in the Figure 5. It is also possible to observe surface delamination in *wet*-conditions. Despite the lubricating effect of water, wear is related to crack growth induced by its tribochemical effects, and possibly due to debris removal by the running water.

5. Conclusions

The new LAS plates, produced by viscous sintering with concurrent crystallisation, and Ceran have similar friction coefficients. The dry tribological tests revealed that the wear rate for the sintered GC is 20% smaller than for the commercial GC Ceran, but in the wet conditions the wear rates are equivalent. The Archard coefficient is slightly smaller for the sintered GC than for the commercial plate under both test conditions.

The main disadvantage of the sinter-crystallisation process is the presence of residual porosity in the material. We verified that despite the fact that the sintered GC has about 5% porosity its mechanical and tribological properties are similar to those of Ceran.

Acknowledgements

The authors are grateful to Brazilian funding agencies CNPq, Capes and FAPESP for their financial support, and Tribology Laboratory at the Universidade Federal do Paraná, for the use of their facilities.

References

1. McMillan, P. W. *Glass Ceramics*. Second edition, Academic Press, London: 1979.
2. Beall, G. H. & Gurney, A. R. *Glass-Ceramic Technology*. The American Ceramic Society: 2002, p. 385.
3. Pannhorst, W. In *Low Thermal Expansion Glass Ceramics*. Edited by H. Bach, Springer, Berlin/Heidelberg/New York, 1995, pp. 1–12.
4. Pannhorst W. Development of the optical glass ceramic Zerodur. In *Low Thermal Expansion Glass Ceramics*. Edited by H. Bach, Springer, Berlin/Heidelberg/New York, 1995, pp. 107–130.
5. Pannhorst, W. Recent developments for commercial applications of low expansion glass ceramics. *Glass Technol,* 2004, **45** (2), 51–3.
6. Zanotto, E. D. A bright future for glass-ceramics. *Am. Ceram. Soc. Bull*., 2010, **89**, 19–27.
7. Müller, G. Structure, composition, stability, and thermal expansion of high-quartz and keatite-type alumino-silicates. In *Low Thermal Expansion Glass Ceramics*. Edited by H. Bach, Springer, Berlin/Heidelberg/New York, 1995, p. 13–24.
8. Naß, P., Rodek, E., Schildt, H. & Weinberg, W. Development and production of transparent colourless and tinted glass ceramics. In *Low Thermal Expansion Glass Ceramics*. Edited by H. Bach, Springer, Berlin/Heidelberg/New York, 1995, p. 60–78.
9. Gutzow, I., Pascova, R., Karamanov, A. & Schmelzer, J. The kinetics of surface induced sinter crystallisation and the formation of glass-ceramic materials. *J. Mater. Sci.*, 1998, **33**, 5265–73.
10. Prado, M. O. & Zanotto, E. D. Glass sintering with concurrent crystallisation. *C. R. Chimie,* 2002, **5**, 773–86.
11. Zanotto, E. D. & Prado, M. O. Isothermal sintering with concurrent crystallisation of monodispersed and polidispersed glass particles: Part 1. *Phys. Chem. Glasses*, 2001, **42** (3), 191–8.
12. Prado, M. O., Zanotto, E. D. & Müller, R. Model for sintering polydispersed glass particles. *J. Non-Cryst. Solids*, 2001, **279**, 169–78.
13. Partridge, G. A. Review of surface crystallisation in vitreous systems. *Glass Technol*., 1987, **28** (1), 9–18.
14. Soares, V. O., Paula, G. R., Peitl Filho, O. & Zanotto, E. D. Effect of ion exchange on the sinter-crystallisation of low expansion $Li_2O–Al_2O_3–SiO_2$ glass-ceramics. *Glass Technol.: Eur. J. Glass Sci. Technol. A*, 2011, **52** (2), 50–4.
15. Serbena, F. C., Soares, V. O., Peitl, O., Pinto, H., Muccillo, R. & Zanotto, E. D. Internal residual stresses in sintered and commercial low expansion $Li_2O–Al_2O_3–SiO_2$ glass-ceramics. *J. Am. Ceram. Soc*., 2011, **94**, 1206–14.
16. Anstis, G. R., Chantikul, P., Lawn, B. R. & Marshall, D. B. A critical evaluation of indentation techniques for measuring fracture toughness: i, direct crack measurements. *J. Am. Ceram. Soc*., 1981, **64**, 533–8.
17. Guille, J. L., Mercier, S. & Hammer, J. M. Determination of the residual stresses in a vitreous enamel by indentation. *J. Mater. Sci. Lett*., 1993, **12**, 1208–9.
18. Zeng, K., Soderlund, E., Giannakopoulos, A. E. & Rowcliffe, D. J. Controlled indentation: a general approach to determine mechanical properties of brittle materials. *Acta Mater*., 1996, **44**, 1127–41.
19. Buchner, S., Mikowski, A., Lepienski, C. M., Ferreira, E. B., Zanotto, E. D., Torres, R. D. & Soares P. Mechanical and tribological properties of a sintered glass-ceramic compared to granite and porcelainized stoneware. *Wear*, 2011, **271**, 875–80.
20. Buchner, S., Lepienski, C. M., Soares Jnr., P. C. & Balzaretti, N. M. Effect of high pressure on the mechanical properties of lithium disilicate glass ceramic. *Mater. Sci. Eng. A*, 2011, **528**, 3921–4.
21. Baker, S. P. In *Encyclopedia of Materials Science and Technology*, Elsevier Science, 2001, pp. 5908.
22. Carlsson, S. & Larsson, P. L. On the determination of residual stress and strain fields by sharp indentation testing. Part I. Theoretical and numerical analysis. *Acta Mater*., 2001, **49**, 2179–91.
23. Oliver, W. C. & Pharr, G. M. An improved technique for determining hardness and elastic modulus using load and displacement sensing indentation experiments. *J. Mater. Res*., 1992, **7** (6), 1564–83.
24. Gant, A. J. & Gee, M. G. Sliding wear corrosion of ceramics. *Wear*, 2009, **267**, 599–607.
25. Michalske, T. A. & Bunker, B. C. The fracturing of glass. *Sci. Am*. 1987, **257**, 122–8.
26. Tomozawa, M. Fracture of glasses. *Ann. Rev. Mater. Sci*., 1996, **26**, 43–74.
27. Clark, D. E., Pantano, Jnr., C. G. & Hench, L. L. *Corrosion of Glass*. Ed. Books for Industry and The Glass Industry. 1979, p. 75.
28. Stachowiak, G. W., Batchelor, A. W. Engineering Tribology, Second ed., Elsevier-Butterworth-Heineman, 2000, 468–78.
29. Blau, P. J., Martin, R. L. & Zanoria, E. S. Effects of surface grinding conditions on the reciprocating friction and wear behaviour of silicon nitride. *Wear*, 1997, **203–204**, 648–57.
30. Jianxin, D., Zeliang, D., Jun, Z., Jianfeng, L. & Tongkun, C. Unlubricated friction and wear behaviors of various alumina-based ceramic composites against cemented carbide. *Ceram. Int*., 2006, **32** (5), 499–507.
31. Bhushan, B. & Gupta, B. K. *Handbook of Tribology: Materials, Coating, and Surface Treatments*. McGraw-Hill, New York, 1991.
32. Archard, J. F. Single contacts multiple encounters. *J. Appl. Phys*., 1961, **32**, 1420–5.
33. Guedes, M., Ferro, A. C. & Ferreira, J. M. F. *J. Eur. Ceram. Soc*., 2001, **21**, 1187–94.
34. Oliver, W. C. & Pharr, G. M. Measurement of hardness and elastic modulus by instrumented indentation: advances in understanding and refinements to methodology. *J. Mater. Res*., 2004, **19** (1), 3–20.
35. Woirgard, J., Tromas, C., Girard, J. C. & Audurier, V. Study of the mechanical properties of ceramic materials by the nanoindentation technique. *J. Eur. Ceram. Soc*., 1998, **18** (15), 2297–305.
36. Lepienski, C. M. & Foerster, C. E. *Encyclopedia of Nanoscience and Nanotechnology*. American Scientific Publishers, Stevenson Ranch, 2004, p. 1–20.
37. Menčík, J. *Uncertainties and Errors in Nanoindentation*. Edited by Dr. Jiri Nemecek, ISBN: 978-953-51-0802-3, InTech, 2012, DOI: 10.5772/50002.
38. Chakraborty, R., Mukhopadhyay, A. K., Joshi, K. D., Rav, A., Mandal, A. K, Bysakh, S, Biswas, S. K. & Gupta, S. C. *Comparative study of indentation size effects in As-sintered alumina and alumina shock deformed at 6·5 and 12 GPa*. International Scholarly Research Network, ISRN Ceramics 2012, 595172, 1–11.
39. Soares, V. O., Peitl, O. & Zanotto, E. D. *J. Am. Ceram. Soc*., 2013, **96** (4), 1143–9.
40. Djelal, C. Designing perfecting a tribometer for the study of friction of a concentrated clay–water mixture against a metallic surface. *Mater. Struct*., 2001, **34**, 51–8.